

# NO CLEAR SUBMILLIMETER SIGNATURE OF SUPPRESSED STAR FORMATION AMONG X-RAY LUMINOUS AGNS

C. M. HARRISON<sup>1</sup>, D. M. ALEXANDER<sup>1</sup>, J. R. MULLANEY<sup>1</sup>, B. ALTIERI<sup>2</sup>, D. COIA<sup>2</sup>, V. CHARMANDARIS<sup>3</sup>, E. DADDI<sup>4</sup>, H. DANNERBAUER<sup>5</sup>, K. DASYRA<sup>6</sup>, A. DEL MORO<sup>1</sup>, M. DICKINSON<sup>7</sup>, R. C. HICKOX<sup>8</sup>, R. J. IVISON<sup>9</sup>, J. KARTALTEPE<sup>7</sup>, E. LE FLOC'H<sup>4</sup>, R. LEITON<sup>4,10</sup>, B. MAGNELLI<sup>11</sup>, P. POPESSO<sup>11</sup>, E. ROVILOS<sup>1</sup>, D. ROSARIO<sup>11</sup>, A. M. SWINBANK<sup>1</sup>

*Draft version April 1, 2024*

## ABSTRACT

Many theoretical models require powerful active galactic nuclei (AGNs) to suppress star formation in distant galaxies and reproduce the observed properties of today's massive galaxies. A recent study based on *Herschel*-SPIRE submillimeter observations claimed to provide direct support for this picture, reporting a significant decrease in the mean star-formation rates (SFRs) of the most luminous AGNs ( $L_X > 10^{44}$  erg s<sup>-1</sup>) at  $z \approx 1-3$  in the *Chandra* Deep Field-North (CDF-N). In this Letter we extend these results using *Herschel*-SPIRE 250  $\mu$ m data in the COSMOS and CDF-S fields to achieve an order of magnitude improvement in the number of sources at  $L_X > 10^{44}$  erg s<sup>-1</sup>. On the basis of our analysis, we find no strong evidence for suppressed star formation in  $L_X > 10^{44}$  erg s<sup>-1</sup> AGNs at  $z \approx 1-3$ . The mean SFRs of the AGNs are constant over the broad X-ray luminosity range of  $L_X \approx 10^{43}-10^{45}$  erg s<sup>-1</sup> (with mean SFRs consistent with typical star-forming galaxies at  $z \approx 2$ ;  $\langle \text{SFRs} \rangle \approx 100-200 \text{ M}_\odot \text{ yr}^{-1}$ ). We suggest that the previous CDF-N results were likely due to low number statistics. We discuss our results in the context of current theoretical models.

*Subject headings:* galaxies: evolution—galaxies: star formation—galaxies: active—X-rays: general

## 1. INTRODUCTION

Over the last decade it has become increasingly clear that active galactic nuclei (AGNs) have had a profound influence on the formation and evolution of galaxies. Some of the most compelling evidence is based on computational simulations and theoretical models, which have shown that AGNs can suppress or shut down star formation by heating, or removing, the cold gas in their host galaxies (e.g., Silk & Rees 1998; Springel et al. 2005; Di Matteo et al. 2005; Bower et al. 2006; Hopkins et al. 2006, 2008; Debuhr et al. 2012). While there is some indirect observational support for the suppression of star formation by AGN activity (see Alexander & Hickox 2012 and Fabian 2012 for general reviews), we currently lack conclusive observational evidence across the overall population.

One approach to assess the influence of AGNs on the growth of galaxies is to explore possible connections between AGN activity and star formation. A large suite of studies have investigated the relationship between AGN activity and star formation out to high redshifts ( $z \approx 3$ ), using deep X-ray and infrared data to constrain the AGN activity and star formation rates (SFRs), respectively (Mullaney et al. 2010; Hatziminaoglou et al. 2010; Lutz et al. 2010; Shao et al. 2010; Mullaney et al. 2012a; Santini et al. 2012; Rosario et al. 2012; Page et al. 2012; Rovilos et al. 2012). These studies have shown that the mean SFRs of moderate-luminosity AGNs ( $L_X \approx 10^{42}-10^{44}$  erg s<sup>-1</sup>) out to  $z \approx 3$  are comparable to those of co-eval star-forming galaxies (e.g., Noeske et al. 2007; Elbaz et al. 2007; Daddi et al. 2007; Pannella et al. 2009). However, while these studies find broadly similar results for the average SFRs of moderate-luminosity AGNs, the picture for luminous AGNs ( $L_X > 10^{44}$  erg s<sup>-1</sup>) is less clear, with the majority of these studies arguing that the mean SFR either rises or remains flat towards the highest luminosities (e.g., Lutz et al. 2010; Shao et al. 2010; Rosario et al. 2012; Rovilos et al. 2012).

Recently, Page et al. (2012) used *Chandra* X-ray and *Herschel*-SPIRE submillimeter data in the *Chandra* Deep Field-North (CDF-N) to report that the mean SFRs of luminous AGNs ( $L_X > 10^{44}$  erg s<sup>-1</sup>) at  $z \approx 1-3$  are significantly lower than those of moderate-luminosity AGNs. The implications of this study are potentially very significant as they imply a direct, empirical connection between luminous AGN activity and the suppression of star formation. However, these results are in disagreement with other studies, many of which also used *Herschel* data in similarly deep fields (e.g., Lutz et al. 2010; Shao et al. 2010; Rosario et al. 2012; Rovilos et al. 2012).

The aim of this Letter is to extend the Page et al.

<sup>1</sup> Department of Physics, Durham University, South Road, Durham DH1 3LE, U.K.

<sup>2</sup> Herschel Science Centre, European Space Astronomy Centre, Villanueva de la Canada, 28691 Madrid, Spain

<sup>3</sup> Department of Physics & Institute of Theoretical and Computation, Physics, University of Crete, 71003 Heraklion, Greece

<sup>4</sup> Laboratoire AIM, CEA/DSM-CNRS-Université Paris Diderot, Irfu/Service d'Astrophysique, CEA-Saclay, Orme des Merisiers, 91191 Gif-sur-Yvette Cedex, France

<sup>5</sup> Universität Wien, Institut für Astrophysik, Türkenschanzstraße 17, A-1180 Wien, Austria

<sup>6</sup> Observatoire de Paris, LERMA (CNRS:UMR8112), 61 Av. de l'Observatoire, F-75014, Paris, France

<sup>7</sup> National Optical Astronomy Observatory, 950 North Cherry Avenue, Tucson, AZ 85719, USA

<sup>8</sup> Department of Physics and Astronomy, Dartmouth College, 6127 Wilder Laboratory, Hanover, NH 03755, USA

<sup>9</sup> UK Astronomy Technology Centre, Royal Observatory, Blackford Hill, Edinburgh EH9 3HJ, UK

<sup>10</sup> Department of Astronomy, Universidad de Concepción, Casilla 160-C, Concepción, Chile

<sup>11</sup> Max-Planck-Institut für Extraterrestrische Physik (MPE), Postfach 1312, 85741, Garching, Germany

(2012) study using *Herschel*-SPIRE 250  $\mu\text{m}$  data in the wider-area COSMOS field, improving the source statistics for  $L_X > 10^{44} \text{ erg s}^{-1}$  AGNs by an order of magnitude. Indeed, a clear limitation of the Page et al. (2012) study was the small number of sources in the  $L_X > 10^{44} \text{ erg s}^{-1}$  bins ( $\approx 7$ –14 objects). We note that our Letter only explores the mean SFRs using stacking analysis and does not explore the individual detection rates (i.e., Figure 1 of Page et al. 2012); however, significant differences in the detection fractions should lead to differences in the mean SFRs. We also repeat our analysis using *Herschel*-SPIRE 250  $\mu\text{m}$  data in the CDF-N and *Chandra* Deep Field South (CDF-S) fields to explore the effect of using smaller fields. In our analysis we use  $H_0 = 71 \text{ km s}^{-1}$ ,  $\Omega_M = 0.27$ ,  $\Omega_\Lambda = 0.73$  and assume a Salpeter initial mass function (IMF).

## 2. CATALOGS AND DATA

### 2.1. X-ray data

Our samples of AGNs are X-ray selected and cover a broad range of luminosities ( $L_X = 10^{42} - 10^{45} \text{ erg s}^{-1}$ ) over the redshift range  $z = 1 - 3$  (see Figure 1). We use the CDF-N (Alexander et al. 2003), CDF-S (Xue et al. 2011) and COSMOS (Elvis et al. 2009) AGN samples to obtain statistically meaningful numbers of AGNs in key  $L_X$  ranges. Redshifts for the CDF-N and CDF-S samples were taken from Bauer et al. in prep. and Xue et al. (2011), respectively. Redshifts for the COSMOS sample were taken from Civano et al. (2012). Unless otherwise stated, we include both photometric and spectroscopic redshifts, which comprise  $\approx 53\%$  and  $\approx 47\%$  of the combined samples respectively; however, we note that our conclusions do not change if we only consider spectroscopic redshifts. Following Page et al. (2012) we derive the rest-frame observed (i.e., not absorption-corrected) 2–8 keV luminosity ( $L_X$ ) of AGNs in each field using  $L_X = 4\pi D^2 F_X (1+z)^{(\Gamma-2)}$ , where  $F_X$  is the observed X-ray flux<sup>12</sup> (2–8 keV),  $D$  is the luminosity distance,  $z$  is the redshift and  $\Gamma$  is the spectral index used for  $k$ -corrections (we assume  $\Gamma = 1.9$ ).

In Figure 1 we show  $L_X$  versus redshift for the X-ray AGNs in each of these fields. These three samples are highly complimentary; the ultra-deep CDF-N and CDF-S samples provide large numbers of moderate luminosity AGNs at  $z = 1 - 3$  (i.e.,  $L_X = 10^{42} - 10^{44} \text{ erg s}^{-1}$ ) while the shallower, wider-area COSMOS survey populates the high-luminosity ( $L_X > 10^{44} \text{ erg s}^{-1}$ ) portion of the parameter space largely missed by these small area surveys.

### 2.2. IR Data

The mean SFRs for our AGN samples are derived from 250  $\mu\text{m}$  observations taken by the SPIRE instrument on board *Herschel* which are relatively unaffected by contamination from the AGN (e.g., Hatziminaoglou et al. 2010) or obscuration due to dust. Our results are primarily based on the observations of the CDF-N, CDF-S and COSMOS fields undertaken as part of the HerMES campaign (P.I.: S. Oliver; described in Oliver et al.

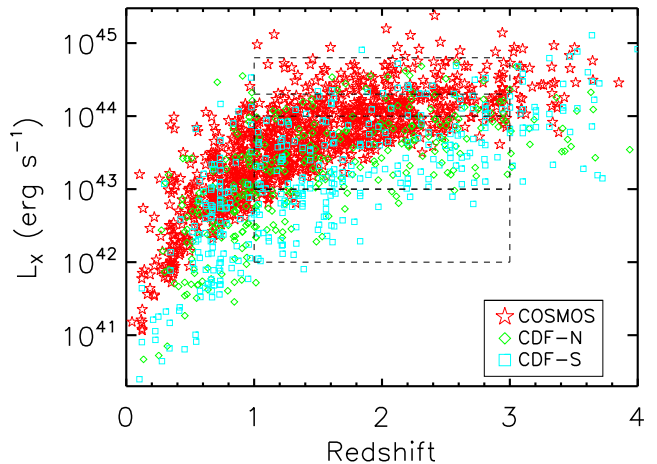


FIG. 1.— Rest-frame 2–8 keV luminosities (not-absorption corrected) of the X-ray AGNs detected in the three deep fields (see §2 for details) versus redshift. The areas of parameter space used in our stacking procedures (see Figure 3) are illustrated with the dashed lines. Caution should be taken when interpreting the lowest X-ray luminosity bin ( $L_X = 10^{42} - 10^{43} \text{ erg s}^{-1}$ ) as it is incomplete at  $z \gtrsim 2$ .

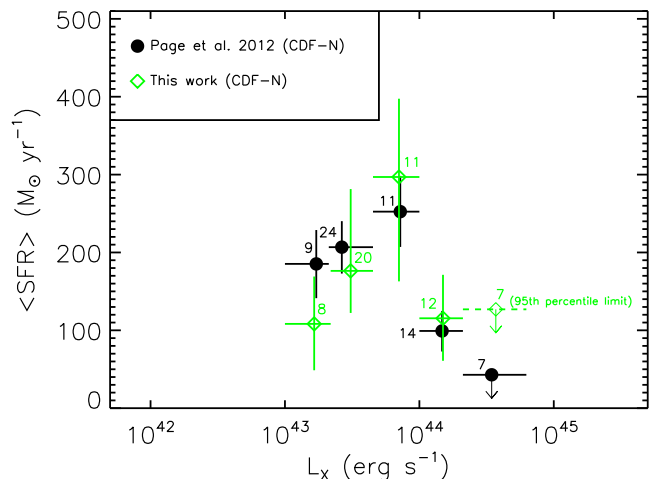


FIG. 2.— Mean star formation rate (SFR) vs. X-ray luminosity for AGNs in the CDF-N field compared to Page et al. (2012); see §3 for details. We find excellent agreement between our mean SFRs and those of Page et al. (2012) across all  $L_X$  bins; we indicate the number of sources in each bin (the differences in the number of objects between our study and Page et al. (2012) are due to differences in the redshift catalogs). We note that for Page et al. (2012) the values were extracted directly from their figures as tabulated values were unavailable. As with Page et al. (2012), we do not measure a significant flux in the highest  $L_X$  bin for which we also include the 95th percentile limit (see §3). This limit is broadly consistent with the mean SFRs for our lower  $L_X$  bins.

2012). We downloaded the individual level-2 data products from each scan of each field (totaling  $\sim 14$  hours,  $\sim 20$  hours and  $\sim 50$  hours in CDF-N, CDF-S and COSMOS, respectively) from the *Herschel* ESA archive and then aligned and coadded the images. The coadded images were then aligned onto a common world co-ordinate system. We also checked for consistency between our own coadds and those produced using the standard HIPE v9.0 pipeline.

We also make use of 250  $\mu\text{m}$  SPIRE observations of the CDF-N field that were undertaken as part of the GOODS-*Herschel* program (GOODS-*H*; P.I.: D. Elbaz) and cover the whole of the CDF-N (totaling 44 hours when combined with the HerMES observations). The

<sup>12</sup> We note Elvis et al. (2009) report 2–10 keV fluxes, which we convert to 2–8 keV fluxes by assuming  $\Gamma = 1.9$  (factor of  $\approx 0.85$  correction).

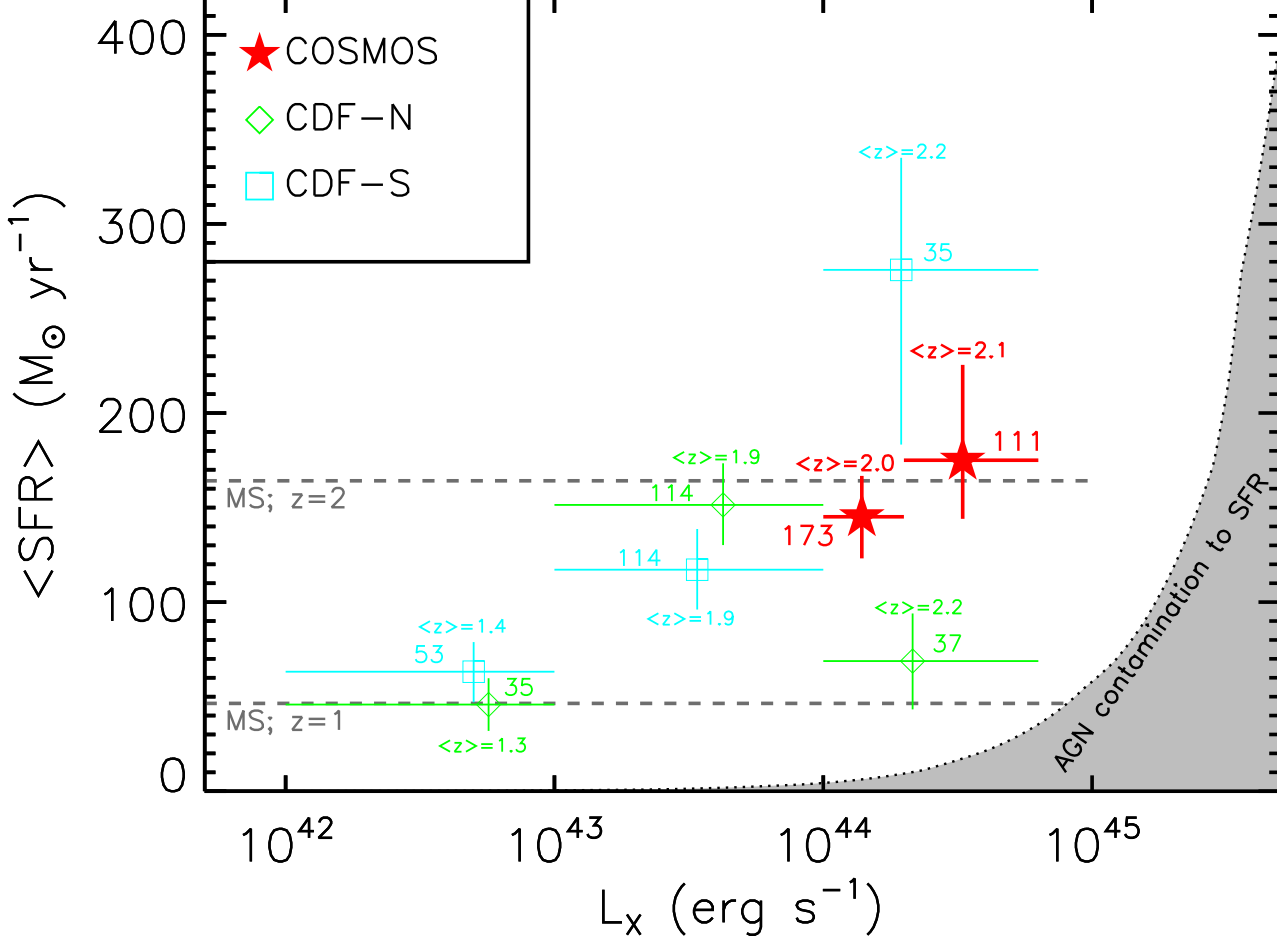


FIG. 3.— Mean SFR vs.  $L_X$  for AGNs in the three fields (see §3 for details). We indicate the number of, and the average redshift of, the AGNs in each bin (Table 1). The dotted curve indicates the contamination to the measured SFR from AGN activity (i.e., the amount that the SFRs will be boosted due to contamination of the  $250\,\mu\text{m}$  flux [rest-frame  $83\,\mu\text{m}$  at  $z = 2$ ] by AGN activity) and is calculated using the  $L_X$ - $L_{\text{MIR}}$  relation of Gandhi et al. (2009) and the intrinsic AGN SED of Mullaney et al. (2011). The dashed lines show the average SFR expected (derived from Elbaz et al. 2011) for a galaxy with a stellar mass of  $9 \times 10^{10} M_\odot$  galaxy, (i.e., about the mean stellar mass of X-ray detected AGN hosts; e.g., Xue et al. 2010; Mullaney et al. 2012a) at  $z = 1.0$  and  $z = 2.0$ . We find that the mean SFR distribution at  $L_X > 10^{42} \text{ erg s}^{-1}$  is roughly equal to that expected from typical star-forming galaxies at the average redshifts of our bins (our  $L_X < 10^{43} \text{ erg s}^{-1}$  bins have lower mean redshifts and hence lower mean SFRs; e.g., Mullaney et al. 2012a). We show that there are variations in the measured mean SFRs between the small CDF-N and CDF-S fields and argue that this, combined with low number statistics drive the Page et al. (2012) results shown in Figure 2.

observations and steps used to produce the science images are described in Elbaz et al. (2011). We note that our results derived from the GOODS-*H* CDF-N observations are consistent with those derived from the HerMES observations of the same field.

### 3. MEASURING AVERAGE STAR FORMATION RATES

To determine the mean SFRs of AGNs as a function of  $L_X$  we split our samples into a number of  $L_X$  bins (see Table 1). The majority of the X-ray AGNs are not individually detected by *Herschel*-SPIRE (e.g., Hatziminaoglou et al. 2010; Page et al. 2012) and therefore, we rely on stacking analysis to obtain the mean  $250\,\mu\text{m}$  fluxes of our AGN samples in each bin. We stack at the optical positions of all X-ray AGNs in our samples, whether they are individually  $250\,\mu\text{m}$ -detected or not (following Page et al. 2012). The point-spread function (PSF) of the SPIRE  $250\,\mu\text{m}$  science images is normalized to 1 and in units of  $\text{mJy beam}^{-1}$ , such that the mean  $250\,\mu\text{m}$  flux was taken to be the central pixel value of each stacked image.

To determine if the measured fluxes from our stacked

images are significantly above the background we employed a Monte-Carlo approach, which quantifies the level of background and confusion noise (i.e., flux contribution to our stacked images from nearby, unassociated sources). First, along with each “true” stacked image we also made 10,000 “random” stacks, stacking the same number of random positions around the field as in our true stacks. The mean flux of the random stacks was subtracted from that of the true stack, effectively removing any systematic contribution from the background or confusion. Second, we compare our measured “corrected” fluxes of our true stacks to the distribution of fluxes from our random stacks. We consider a stacked signal to be significant if the flux is greater than the flux of 95% of the random trials. Following this criterion, all but one of our stacked images have flux measurements that are significant (see §4 for details). We note that this method of randomly choosing positions to estimate the background does not take into account any clustering between X-ray AGNs and IR-sources (this was also not considered in Page et al. 2012). While this will not affect the SFR- $L_X$  trends, the mean background subtracted from each

TABLE 1  
DERIVED AVERAGE PROPERTIES OF SUB-SAMPLES

$L_X$ range	$N_{\text{AGN}}$	$\langle z \rangle$	$\langle L_X \rangle$	$\langle S_{250} \rangle$	$\langle \text{SFR} \rangle$
(1)	(2)	(3)	(4)	(5)	(6)
CDF-N (HerMES; Figure 2)*					
43.00 – 43.33	8	1.8	43.2	$5.4^{+3.0}_{-3.0}$	$108^{+61}_{-60}$
43.33 – 43.66	20	1.7	43.5	$9.4^{+2.3}_{-2.4}$	$176^{+105}_{-54}$
43.66 – 44.00	11	1.9	43.8	$10.9^{+3.7}_{-3.6}$	$297^{+100}_{-134}$
44.00 – 44.33	12	2.0	44.2	$4.8^{+2.5}_{-2.4}$	$115^{+56}_{-55}$
44.33 – 44.80	7	2.1	44.6	<4.4	< 127
CDF-N (GOODS- $H$ ; Figure 3)					
42.00 – 43.00	35	1.3	42.8	$3.5^{+1.1}_{-1.1}$	$46^{+14}_{-14}$
43.00 – 44.00	114	1.9	43.6	$6.8^{+1.0}_{-0.9}$	$151^{+22}_{-21}$
44.00 – 44.80	37	2.2	44.3	$2.2^{+0.9}_{-0.9}$	$69^{+25}_{-26}$
CDF-S (Figure 3)					
42.00 – 43.00	53	1.4	42.7	$4.3^{+1.0}_{-1.1}$	$63^{+16}_{-16}$
43.00 – 44.00	114	1.9	43.5	$5.3^{+1.0}_{-1.0}$	$117^{+22}_{-21}$
44.00 – 44.80	35	2.2	44.3	$7.2^{+1.4}_{-1.4}$	$276^{+59}_{-92}$
COSMOS (Figure 3)					
44.00 – 44.30	173	2.0	44.1	$6.0^{+0.9}_{-0.9}$	$145^{+22}_{-22}$
44.30 – 44.80	111	2.1	44.5	$6.3^{+1.1}_{-1.1}$	$175^{+50}_{-31}$

NOTE. — (1) X-ray luminosity (2–8 keV) range of each bin ( $\log[\text{erg s}^{-1}]$ ); (2) Number of X-ray AGNs in each bin; (3) Mean redshift; (4) Mean  $L_X$  ( $\log[\text{erg s}^{-1}]$ ); (5) Mean 250  $\mu\text{m}$  flux and uncertainties (mJy); (6) Mean star formation rate ( $\text{M}_\odot \text{ yr}^{-1}$ ). The quoted uncertainties are derived from our bootstrap method (see §3). \*To be consistent with Page et al. (2012) we use the same  $L_X$  bins and only include AGNs with spectroscopic redshifts when stacking the HerMES data for the CDF-N field (see §4).

stacked image may be slightly under-estimated, resulting in the absolute mean SFRs quoted being slightly over-estimated. However, we note that our results are consistent with studies that are less affected by confusion noise (e.g., Mullaney et al. 2012a; Rosario et al. 2012), giving confidence in our procedures.

We used the spectral energy distribution (SED) library of Chary & Elbaz (2001) to convert mean 250  $\mu\text{m}$  fluxes from our stacked images to mean integrated 8–1000  $\mu\text{m}$  infrared luminosities ( $L_{\text{IR}}$ ), selecting a redshifted Chary & Elbaz (2001) SED on the basis of the monochromatic luminosity probed by the 250  $\mu\text{m}$  waveband. These mean  $L_{\text{IR}}$  values were converted to mean SFRs using Kennicutt (1998). In the redshift range  $z=1$ –3 investigated here, the observed 250  $\mu\text{m}$  fluxes correspond to the peak of the SEDs in the rest frame. As such the  $L_{250}$  to  $L_{\text{IR}}$  correction factors do not vary much as a function of SED shape when compared to using shorter wavelengths (see Figure 3 in Elbaz et al. 2010). Indeed, when we compared *all* of the Chary & Elbaz (2001) SEDs, redshifted to  $z=2$ , the conversion factors were consistent within  $\approx 20\%$ ; we also repeated our analysis using the main-sequence SED from Elbaz et al. (2011) for all of the bins and found no significant difference. While the choice of SED adds a small additional uncertainty in the measured SFRs (such that quoted absolute SFRs should be used with care), all of the observed trends, and hence the main conclusions of this Letter, remain unaffected. We also show in §4 that we reproduce the results of Page et al. (2012), providing further

confidence in our approach.

Upper and lower limits on the mean SFRs for each of our  $L_X$  bins were calculated using a bootstrapping technique, therefore taking into account the distribution of SFRs in each stack. We randomly subsample (with replacement) the AGNs in each of our bins, restack and recalculate the mean SFR. We did this 10,000 times for each bin to produce a distribution of mean SFRs. The quoted upper and lower limits on the mean SFRs correspond to the 16th and 84th percentiles (i.e., incorporating 68%, or  $\approx \pm 1\sigma$ ) of this distribution (Table 1).

#### 4. RESULTS AND DISCUSSION

We first stacked sub-samples of X-ray AGNs in the CDF-N. In an attempt to reproduce the results of Page et al. (2012) we split the sample into the same luminosity bins used in their study (Table 1) and only included AGNs with spectroscopic redshifts; see Figure 2. We find excellent agreement between our mean SFRs and those of Page et al. (2012) (i.e., data points are consistent within their uncertainties), demonstrating the compatibility of the procedures used to derive these results.<sup>13</sup> In agreement with Page et al. (2012), we do not obtain a significant flux measurement from the stacked 250  $\mu\text{m}$  image of our highest  $L_X$  bin ( $\log[L_X/\text{erg s}^{-1}] = 44.33 - 44.80$ ). However, unlike Page et al. (2012), we find our upper limit is consistent with the mean SFRs of the lowest  $L_X$  bins.

The non-detection at FIR wavelengths of the AGNs in our highest  $L_X$  bin in the CDF-N field, combined with the small numbers of AGNs in this bin (7 sources), clearly demonstrates the need for larger numbers of sources at high X-ray luminosities. To achieve this we performed the same stacking procedures using the COSMOS survey. The inclusion of the COSMOS AGNs means that the number of sources in our highest  $L_X$  bins are now greater by an order of magnitude (Figure 1 and Table 1). As such, we can now place tighter constraints on the mean SFRs of high-luminosity AGNs. On the basis of our stacking analysis in the COSMOS field, we find that the mean SFRs of AGNs with  $L_X > 10^{44} \text{ erg s}^{-1}$  are consistent with those of  $L_X = 10^{43}$ – $10^{44} \text{ erg s}^{-1}$  AGNs ( $\approx 100$ – $200 \text{ M}_\odot \text{ yr}^{-1}$ ; see Figure 3 and Table 1). This implies that the mean SFR of  $z=1$ –3 AGNs is independent of X-ray luminosity (although increases with increasing redshifts), in broad agreement with Rosario et al. (2012) and indicates that the flat SFR distribution at  $L_X < 10^{44} \text{ erg s}^{-1}$  (e.g., Lutz et al. 2010; Shao et al. 2010; Mullaney et al. 2012a; Rosario et al. 2012) continues out to at least  $L_X \approx 10^{44.8} \text{ erg s}^{-1}$ .<sup>14</sup>

The results derived from our stacking of AGNs in the COSMOS field may suggest that poor source statistics and potentially field-to-field variations (i.e., cosmic variance) are at least partially responsible for the disagreement between the results from COSMOS and CDF-N at high X-ray luminosities. To further investigate this we also stacked the SPIRE data in the CDF-S field,

<sup>13</sup> We note that Page et al. (2012) used a different technique to that adopted by us here; they derive average SFRs by fitting a modified black body to the SPIRE fluxes of each source.

<sup>14</sup> We note that this approach is different to averaging over *all*  $L_X$  and  $L_{\text{IR}}$  over *all* star-forming galaxies (whether X-ray detected or not) where a clear relationship between  $L_X$  and SFR is found (see Mullaney et al. 2012b).

which is of a similar size as the CDF-N and contains approximately the same number of high  $L_X$  AGNs (Figure 1). We also restack the CDF-N AGNs using the deeper 250  $\mu\text{m}$  observations taken as part of the GOODS-*H* program since this is of comparable depth to the HerMES CDF-S observations. As shown in Figure 3, we find broad agreement between the mean SFRs of moderate luminosity AGNs (i.e.,  $L_X < 10^{44} \text{ erg s}^{-1}$ ) in both fields: the mean SFRs with X-ray luminosity over the range  $L_X \approx 10^{42} - 10^{44} \text{ erg s}^{-1}$  are consistent with those expected from typical star-forming galaxies with the average redshifts and typical stellar masses observed for the AGN host galaxies. The increasing specific SFRs with redshift (e.g., Elbaz et al. 2011) is likely to drive the apparent increase in the mean SFRs between  $L_X \approx 10^{42} - 10^{43} \text{ erg s}^{-1}$  and  $L_X \approx 10^{43} - 10^{44} \text{ erg s}^{-1}$  (i.e., they have different mean redshifts).

In contrast to the lower X-ray luminosity systems, the mean SFRs of AGNs between CDF-N and CDF-S appears to diverge at the highest X-ray luminosities (i.e.,  $L_X > 10^{44} \text{ erg s}^{-1}$ ). We note that the higher mean SFR observed for high  $L_X$  AGNs in the CDF-S is broadly consistent with the results found by Lutz et al. (2010) and Rovilos et al. (2012) in the same field. Despite these field-to-field variations the mean SFRs in the CDF-S and CDF-N fields are consistent with that found in the COSMOS field (within  $\approx 1\sigma$  and  $\approx 3\sigma$  respectively).

We now consider if our main result indicates that luminous AGN activity does not suppress star formation in the host galaxies. Any *observed* change in the mean SFRs due to luminous AGN activity will depend on the relative timescales of the process of shutting down star formation and of the luminous AGN activity itself. For example, if the time between the onset of luminous AGN activity and the shut down of star formation is longer than the AGN lifetime (which may in itself be highly variable; e.g., Novak et al. 2011) then it would be challenging to observe significantly reduced mean SFRs, simply on the basis of an X-ray luminosity threshold. A major uncertainty in providing a detailed assessment of possible con-

nections between luminous AGNs and the suppression of star formation is due to the relative lifetimes of these processes. Modeling suggests that episodes of the most luminous AGN activity last  $< 80 \text{ Myrs}$  (Hopkins et al. 2005; Novak et al. 2011) while studies based on black hole mass functions and AGN luminosity functions imply that luminous AGN activity could last in excess of  $\approx 10^8$  years (e.g. Marconi et al. 2004; Kelly et al. 2010; Cao 2010). Observations of AGN-driven  $\approx 1000 \text{ km s}^{-1}$  outflows, found over kilo-parsec scales in  $z \approx 1-3$  ultra-luminous infrared galaxies (ULIRGs; Harrison et al. 2012) indicate that star-formation episodes could be rapidly shut down; indeed, detailed studies of local ULIRGs with AGN-driven molecular outflows indicate that their gas reservoirs could be completely removed in  $\approx 1-40 \text{ Myrs}$  (e.g., Feruglio et al. 2010; Sturm et al. 2011). Therefore, while to first order our results may appear to suggest that luminous AGNs do not suppress star formation, it is also possible that the timescales for luminous AGN activity and the suppression of star-formation are comparable, meaning that any signatures of suppression would be very challenging to detect with the current data. Clearer signatures of suppressed star formation may be more apparent when considering subsets of the AGN population which may represent specific evolutionary stages (e.g., Page et al. 2004; Stevens et al. 2005).

To summarize, we find no evidence for the significantly reduced mean SFRs among high luminosity AGNs, and the mean SFRs measured are consistent with that expected from typical star-forming galaxies at the average redshifts and typical stellar masses of our bins. We have suggested that depending on the timescales involved, it could be challenging to see the signature of suppressed star formation simply on the basis of an X-ray luminosity threshold.

We acknowledge the STFC (CMH; DMA; ADM and AMS), the Leverhulme Trust (JRM) and NASA (MD and JK). We thank the anonymous referee, Douglas Scott and Mat Page for useful comments. This research made use of data from the HerMES project (Oliver et al. 2012) which utilizes the *Herschel* ESA space observatory.

## REFERENCES

- Alexander, D. M., & Hickox, R. C. 2012, *NewAR*, 56, 93  
 Alexander, D. M., Bauer, F. E., Brandt, W. N., et al. 2003, *AJ*, 126, 539  
 Bower, R. G., Benson, A. J., Malbon, R., et al. 2006, *MNRAS*, 370, 645  
 Cao, X. 2010, *ApJ*, 725, 388  
 Chary, R., & Elbaz, D. 2001, *ApJ*, 556, 562  
 Civano, F., Elvis, M., Brusa, M., et al. 2012, *ApJS*, 201, 30  
 Daddi, E., Dickinson, M., Morrison, G., et al. 2007, *ApJ*, 670, 156  
 Debuhr, J., Quataert, E., & Ma, C.-P. 2012, *MNRAS*, 420, 2221  
 Di Matteo, T., Springel, V., & Hernquist, L. 2005, *Nature*, 433, 604  
 Elbaz, D., Daddi, E., Le Borgne, D., et al. 2007, *A&A*, 468, 33  
 Elbaz, D., Hwang, H. S., Magnelli, B., et al. 2010, *A&A*, 518, L29  
 Elbaz, D., Dickinson, M., Hwang, H. S., et al. 2011, *A&A*, 533, A119  
 Elvis, M., Civano, F., & Vignali et al., C. 2009, *ApJS*, 184, 158  
 Fabian, A. C. 2012, *ARA&A*, 50, 455  
 Feruglio, C., Maiolino, R., Piconcelli, E., et al. 2010, *A&A*, 518, L155  
 Gandhi, P., Horst, H., Smette, A., et al. 2009, *A&A*, 502, 457  
 Harrison, C. M., Alexander, D. M., Swinbank, A. M., et al. 2012, *MNRAS*, 426, 1073  
 Hatziminaoglou, E., Omont, A., Stevens, J. A., et al. 2010, *A&A*, 518, L33  
 Hopkins, P. F., Hernquist, L., Cox, T. J., et al. 2005, *ApJ*, 630, 716  
 —. 2006, *ApJS*, 163, 1  
 Hopkins, P. F., Hernquist, L., Cox, T. J., & Kereš, D. 2008, *ApJS*, 175, 356  
 Kelly, B. C., Vestergaard, M., Fan, X., et al. 2010, *ApJ*, 719, 1315  
 Kennicutt, Jr., R. C. 1998, *ARA&A*, 36, 189  
 Lutz, D., Maimieri, V., Rafferty, D., et al. 2010, *ApJ*, 712, 1287  
 Marconi, A., Risaliti, G., Gilli, R., et al. 2004, *MNRAS*, 351, 169  
 Mullaney, J. R., Alexander, D. M., Goulding, A. D., & Hickox, R. C. 2011, *MNRAS*, 414, 1082  
 Mullaney, J. R., Alexander, D. M., Huynh, M., Goulding, A. D., & Frayer, D. 2010, *MNRAS*, 401, 995  
 Mullaney, J. R., Pannella, M., Daddi, E., et al. 2012a, *MNRAS*, 419, 95  
 Mullaney, J. R., Daddi, E., Béthermin, M., et al. 2012b, *ApJ*, 753, L30  
 Noeske, K. G., Weiner, B. J., Faber, S. M., et al. 2007, *ApJ*, 660, L43  
 Novak, G. S., Ostriker, J. P., & Ciotti, L. 2011, *ApJ*, 737, 26  
 Oliver, S. J., Bock, J., Altieri, B., et al. 2012, *MNRAS*, 424, 1614

- Page, M. J., Stevens, J. A., Ivison, R. J., & Carrera, F. J. 2004, *ApJ*, 611, L85
- Page, M. J., Symeonidis, M., Vieira, J. D., et al. 2012, *Nature*, 485, 213
- Pannella, M., Carilli, C. L., Daddi, E., et al. 2009, *ApJ*, 698, L116
- Rosario, D. J., Santini, P., Lutz, D., et al. 2012, *A&A*, 545, A45
- Rovilos, E., Comastri, A., Gilli, R., et al. 2012, *A&A*, 546, A58
- Santini, P., Rosario, D. J., Shao, L., et al. 2012, *A&A*, 540, A109
- Shao, L., Lutz, D., Nordon, R., et al. 2010, *A&A*, 518, L26
- Silk, J., & Rees, M. J. 1998, *A&A*, 331, L1
- Springel, V., Di Matteo, T., & Hernquist, L. 2005, *MNRAS*, 361, 776
- Stevens, J. A., Page, M. J., Ivison, R. J., et al. 2005, *MNRAS*, 360, 610
- Sturm, E., González-Alfonso, E., Veilleux, S., et al. 2011, *ApJ*, 733, L16
- Xue, Y. Q., Luo, B., Brandt, W. N., & Bauer et al., F. E. 2011, *ApJS*, 195, 10
- Xue, Y. Q., Brandt, W. N., Luo, B., et al. 2010, *ApJ*, 720, 368